

Oxidation by molecular oxygen using zeolite encapsulated Co(II)saloph complexes

Trissa Joseph, S.B. Halligudi*, C. Satyanarayan,
Dhanashree P. Sawant, S. Gopinathan

Inorganic Chemistry and Catalysis Division, National Chemical Laboratory, Pune 411008, India

Received 29 May 2000; accepted 19 September 2000

Abstract

Co(II) Schiff base complexes encapsulated in zeolite-Y having the general formula Co(II)L-Y (where L = salicylaldehyde-*o*-phenylenediimine (saloph), chloro-salicylaldehyde-*o*-phenylenediimine (Cl-saloph), bromo-salicylaldehyde-*o*-phenylenediimine, (Br-saloph) and nitro-salicylaldehyde-*o*-phenylenediimine, (nitro-saloph) and Y = zeolite Na-Y) have been synthesized and characterized for their physicochemical and spectroscopic properties. The neat and encapsulated catalysts were tested for their catalytic activities in the oxidation of β -isophorone (BIP) to keto-isophorone (KIP) using air as an oxidant at ambient conditions of pressure and temperature. It was found that the catalytic activities of encapsulated catalysts were higher than their homogeneous analogues in the oxidation reaction. Among the catalysts, however, Co(II)Cl-saloph neat and its encapsulated forms were comparatively more active than other catalysts tested in the oxidation reaction. The catalytic activities of neat and their encapsulated forms followed the same trend and the order of reactivities were: Co(II)Cl-saloph > Co(II)Br-saloph > Co(II)nitro-saloph > Co(II)saloph. Kinetics of Co(II)Cl-saloph-Y catalyzed aerial oxidation of BIP was investigated and the rates of oxidation have been obtained for variations made in catalyst, substrate and oxidant concentrations. Mechanism of oxidation involving Co(III)–O–O[•] superoxo intermediate species in the oxidation of BIP has been established by UV–VIS using Co(II)saloph neat complex. Effect of temperature on the rates of oxidation of BIP was also studied and from Arrhenius plot, thermodynamic activation parameters estimated have been reported. © 2001 Elsevier Science B.V. All rights reserved.

Keywords: Co(II)saloph complexes; Zeolite-Na-Y; Catalysts; Oxidation; β -Isophorone; Kinetics; Mechanism; Superoxo

1. Introduction

Heterogenization of homogeneous catalysts has been an interesting area of research and from the industrial point of view, this could provide an ideal method for combining the advantages and simulta-

neously avoiding the disadvantages of homogeneous and heterogeneous catalysts [1–3]. Zeolites such as faujasite (Na-Y and Na-X), which are microporous materials having the cage size (1.2 nm) and a 3D chamber with SiO₂:Al₂O₃ = 3–5, have been used extensively in the preparation of zeolite encapsulated transition metal complex catalysts [4–11]. The microporous and ordered channels in zeolites could be regarded as “nanometric-sized microreactors”. These catalysts could be easily prepared by the exchange

* Corresponding author. Tel.: +91-20-5893300/ext. 2000;
fax: +91-20-5411696.
E-mail address: halligudi@cata.ncl.res.in (S.B. Halligudi).

of transition metal salts with Na^+ of zeolite-Y or X and then treated with ligands (flexible ligand method) or preparation of metal complex surrounding zeolite moiety to give zeolite encapsulated metal complex (ZEMC) catalysts. These encapsulated metal complexes become too large and rigid to escape out of the zeolite cages (ship-in-bottle) and, thus, provide chemically and structurally controllable surface systems for applications in catalysis.

ZEMC catalysts provide many novelties for the development of selective liquid phase oxidation of hydrocarbons to oxygenated products. These catalysts behave functionally similar to many enzyme catalyzed oxidation reactions (zeozymes). Site isolation of metals in inorganic matrices gives unique activities, such as, regio-, enantio- and shape-selectivities, because of the environment surrounding the molecular geometry of metal complexes in zeolite cages. ZEMC catalysts sometimes show higher catalytic activities than their homogeneous analogues in many catalytic transformations.

V(O)Salen encapsulated in Na-Y zeolite has been reported as a catalyst for the epoxidation of cyclohexene to cyclohexeneoxide [4]. Our group has reported that the oxidation of *p*-cresol catalyzed by Co(II)Salen-zeolite-Y gave *para*-hydroxy benzaldehyde [12] and Mn(III)Salen and Mn(II)Salen-Y catalyzed the oxidation of β -isophorone (BIP) to keto-isophorone (KIP) under milder reaction conditions [13,14]. In literature, many reports have appeared on the above topic and still this area is under innovation. Hence, this is a promising field of research to develop efficient ZEMC catalysts for some of the industrially important reactions, where cost and environmental aspects are of importance for any process to be commercially successful.

In continuation of our activities in this area and keeping in view of the above goals, we are reporting in this paper our findings on the synthesis, physicochemical and spectroscopic properties and catalytic activities in aerobic oxidation of BIP to KIP by Co(II)saloph-Y and its neat derivatives containing substituted electron withdrawing groups, such as, $-\text{Cl}$, $-\text{Br}$ or $-\text{NO}_2$ in saloph ligand. BIP to KIP is an important reaction, since, KIP is used for producing compounds of Vitamin A, E series and hence, the above study has been aimed at provid-

ing a heterogeneous catalyst systems for the above reaction.

2. Experimental

2.1. Materials

Zeolite-Y, salicylaldehyde, 5-chloro-salicylaldehyde, 5-bromo-salicylaldehyde, and 5-nitro-salicylaldehyde and *o*-phenylenediimine were procured from M/s. Aldrich Chemicals Co., USA. $\text{Co}(\text{OAc})_2 \cdot 4\text{H}_2\text{O}$ and ethanol were procured from M/s. SISCO Research Laboratories Pvt. Ltd., Mumbai and double distilled water was used in the experiments. M/s. Herdillia, Mumbai, provided BIP and KIP. Triethyl amine, acetyl acetate, methylethyl ketone (MEK), acetonitrile and *t*-butyl alcohol used were of high purity and used as such in the catalytic experiment.

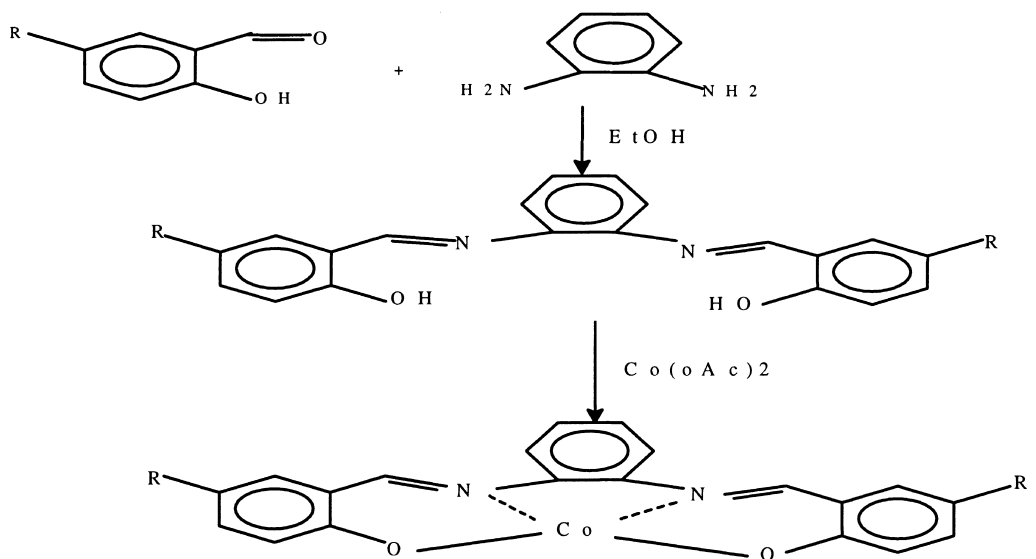
2.2. Catalysts preparation

2.2.1. Synthesis of Co(II)-Y

$\text{Co}(\text{OAc})_2 \cdot 4\text{H}_2\text{O}$ (3.5 g) was dissolved in warm distilled water (700 ml) to which zeolite Na-Y (7.5 g) was added and the contents were refluxed for 8 h. A pink colored solid obtained was collected by filtration and this solid was washed several times with hot water. The cobalt-exchanged zeolite was dried in air overnight at 383 K in an oven and used in the preparation of catalysts.

2.2.2. Preparation of salicylaldehyde-*o*-phenylenediimine (saloph) ligand

The stoichiometric amount of salicylaldehyde (2.44 g) dissolved in ethanol (25 ml) is added drop by drop to *ortho*-phenylene diamine solution (1.08 g in 25 ml ethanol). The contents were refluxed for 3 h and a bright yellow precipitate of saloph was obtained. The yellow precipitate was separated by filtration, washed and dried in vacuum. It was then recrystallized from ethanol to yield saloph (3.0 g). Similarly, Cl-saloph, Br-saloph and nitro-saloph ligands were prepared by using the corresponding salicylaldehyde derivatives. Elemental and spectroscopic analysis of neat complexes confirmed the molecular composition of ligands. The schematic representation of the



Where, $R = H$, Saloph, $R = Cl$, *cl*-Saloph
 $R = Br$, *br*-Saloph, $R = NO_2$, *nito*-Saloph

Scheme 1: Preparation of Co(II)Saloph catalysts

Scheme 1. Preparation of Co(II)saloph catalysts.

method of preparation of ligands and complexes is as shown in Scheme 1.

2.2.3. Preparation of Co(II)saloph

Cobaltous acetate (0.83 g) and saloph (1.05 g) were dissolved in ethanol (25 ml) and refluxed for 3 h. On cooling the reaction mixture, dark brown crystals of Co(II)saloph were obtained (1.5 g). Similarly, Co(II)Cl-saloph, Co(II)Br-saloph and Co(II)nitro-saloph were prepared by the interaction of cobaltous acetate with the corresponding ligands. Elemental and spectroscopic analysis confirmed the composition of these metal complexes and the schematic reaction is as shown in Scheme 1.

2.2.4. Synthesis of Co(II)saloph-Y by flexible ligand method

Saloph (0.4 g) was dissolved in 80 ml of *t*-butyl alcohol and to it Co(II)-Y (2.0 g) was added and this mixture was stirred for 16 h at 323–330 K. The resulting slurry was filtered and the solid was Soxhlet extracted for 48 h with *t*-butyl alcohol. This solid was

further refluxed with 1 M NaCl (50 ml) solution for 16 h to replace the uncomplexed Co(II) ions adhering to the outer surface of zeolite by Na^+ . After this, the solid product was filtered and washed with hot water to remove the adsorbed chloride ions (silver nitrate test). The above product was then dried at 383 K for 6 h and the dirty brown solid retained its color even after Soxhlet extraction with acetonitrile. This indicated the retention of complex inside the zeolite super cages.

When the complex was deposited on the external surface of the zeolite by impregnation method, and when it was Soxhlet extracted with acetonitrile, the zeolite regained its white color, indicating the complete removal of complex from the external surface of zeolite by acetonitrile. These experiments indicated the location of complex inside the pores of the zeolite and not on the external surface. This was verified in our preparation of exchanged complexes in zeolite-Y. Similarly, other substituted salophs, Co(II)Cl-saloph-Y, Co(II)Br-saloph-Y and Co(II)nitro-saloph-Y catalysts were also prepared by treating Co(II)-Y with respective ligands by following the above procedure.

2.3. Characterization of catalysts

The C, H, N analysis of the neat complexes was obtained from Carlo ERBA (Italy) Model EA 1108 analyzer. The electronic spectra of the neat complexes were taken on a Shimadzu UV–VIS scanning spectrophotometer (Model 2101 PC). FTIR spectra of the solid samples were recorded on a Shimadzu FTIR instrument (Model 8201PC). Powder X-ray diffraction of the zeolite encapsulated metal complex catalysts were carried out using a Rigaku (Model D/MAXIII VC, Japan), set-up with Cu K α radiation and a graphite monochromatic with scan speed 16°/min and scanning in the 2 θ range from 5 to 50°. Silicon was used to calibrate the instrument. The cobalt content of the samples was measured by atomic absorption spectrometer (AAS-Hitachi Model Z-8000). Surface area and pore volume of the zeolite-encapsulated catalysts were determined by Omnisorb 100 CX (Coulter, USA).

2.4. Catalytic activity measurements

Experiments were carried out in a two-necked round bottom flask fitted with a water condenser connected to a balloon filled-with air and kept in a thermostatic oil bath. Reaction mixture containing known amounts of BIP, catalyst, MEK solvent (excess), small amounts of acetyl acetate and trimethyl amine (additives) was placed into the flask. The flask was then flushed twice with air before it was finally connected to balloon filled with air. The reaction was initiated by stirring the reaction mixture with a magnetic needle and samples withdrawn at regular intervals of time were analyzed by gas chromatography (Shimadzu 14B) using

FID detector and a capillary column. From GC analysis, the conversions of BIP were calculated and KIP was obtained as the major product of oxidation under the reaction conditions studied and its identity was confirmed by GC–MS (Shimadzu GCMS QP 5000).

3. Results and discussion

3.1. Chemical analysis

The cobalt content of the ZEMC catalysts were estimated by dissolving the known amounts of the catalyst in concentrated HCl and from these solutions, cobalt contents were estimated by atomic absorption spectrometer. The cobalt content of the different catalysts synthesized were almost the same in all the encapsulated systems and were in the range 1.0–1.2 wt.%.

3.2. IR spectroscopy

IR spectra of neat as well as encapsulated complexes gave information on the stretching vibration of the functional groups, the environment of the complex and the crystallinity of the zeolite. The IR spectra of complexes show a shift in the ν C=N to a lower frequency compared to free ligands. This shift is characteristic of coordination of azomethine nitrogen to cobalt as a result of complex formation. The IR bands of all encapsulated complexes are weak due to their low concentration in the zeolite cages. The IR spectra of these catalysts show major bands around 1608, 1571, 1508, 1456, 1355 and 1141 cm^{-1} and the values for different catalysts are presented in Table 1.

Table 1
IR spectra (cm^{-1}) of the neat and encapsulated complexes^a

Catalyst	ν C=C	ν C–H	ν C=N	ν C–N	ν C–O	Ring vibrations
Co(II)L	1610(s)	2923(vs), 2854(s)	1581(m)	1184(s)	1028(s)	1410(s), 1109(w), 746(s)
Co(II)L-Y	1602(m)	2910(m), 2849(m)	1572(w)	1181(m)	1035(m)	1400(s), 1082(w), 754(w)
Co(II)Cl-L	1602(s)	2854(vs), 2322(m)	1570(s)	1178(s)	1049(s)	1406(s), 1082(s), 756(s)
Co(II)Cl-L-Y	1608(m)	2879(m), 2898(m)	1572(s)	1179(m)	1080(w)	1456(s), 1110(m), 765(w)
Co(II)Br-L	1600(s)	2890(s), 2900(m)	1558(s)	1165(s)	1049(m)	1400(s), 1070(s), 754(s)
Co(II)Br-L-Y	1600(m)	2898(m), 2880(m)	1571(m)	1141(m)	1041(w)	1456(s), 1060(m), 808(w)
Co(II)nitro-L	1598(s)	2880(vs), 2941(m)	1562(s)	1151(s)	1049(m)	1457(s), 1080(s), 760(s)
Co(II)nitro-L-Y	1600(s)	2882(m), 2936(m)	1560(w)	1155(m)	1065(w)	1460(s), 1071(s), 775(m)

^a L = saloph; w = weak; s = strong; vs = very strong; m = medium.

Table 2
Surface area and pore volume of catalysts

Catalyst	Surface area (m ² /g)	Macro pore volume (ml/g)
Na-Y	836.3	0.4234
Co-Y	554.0	0.2323
Co(II)Cl-saloph-Y	484.9	0.2027
Co(II)Br-saloph-Y	475.7	0.2050
Co(II)nitro-saloph-Y	369.2	0.1710
Co(II)saloph-Y	442.9	0.2147

3.3. Diffuse reflectance spectra

The diffuse reflectance spectra of Co(II) complexes containing saloph and substituted saloph complexes were almost identical before and after encapsulation, indicating the complexes maintain their geometry even after encapsulation without significant distortion.

3.4. Surface area and pore volume

The surface area and pore volume of the catalysts is presented in Table 2. The encapsulation of Co(II)saloph complexes in zeolite reduced the adsorption capacity and the surface area of the zeolite. The lowering of the pore volume and surface area indicated the presence of Co(II)saloph complexes within the zeolite cages and not on the external surface.

3.5. X-ray diffraction

The X-ray diffractograms of the zeolite encapsulated catalysts containing Co(II) complexes are shown in Fig. 1. The X-ray diffractograms of zeolite encapsulated Co(II)saloph catalysts did not reveal any significant difference from those of Na-Y except a slight decrease in the intensities of the peaks.

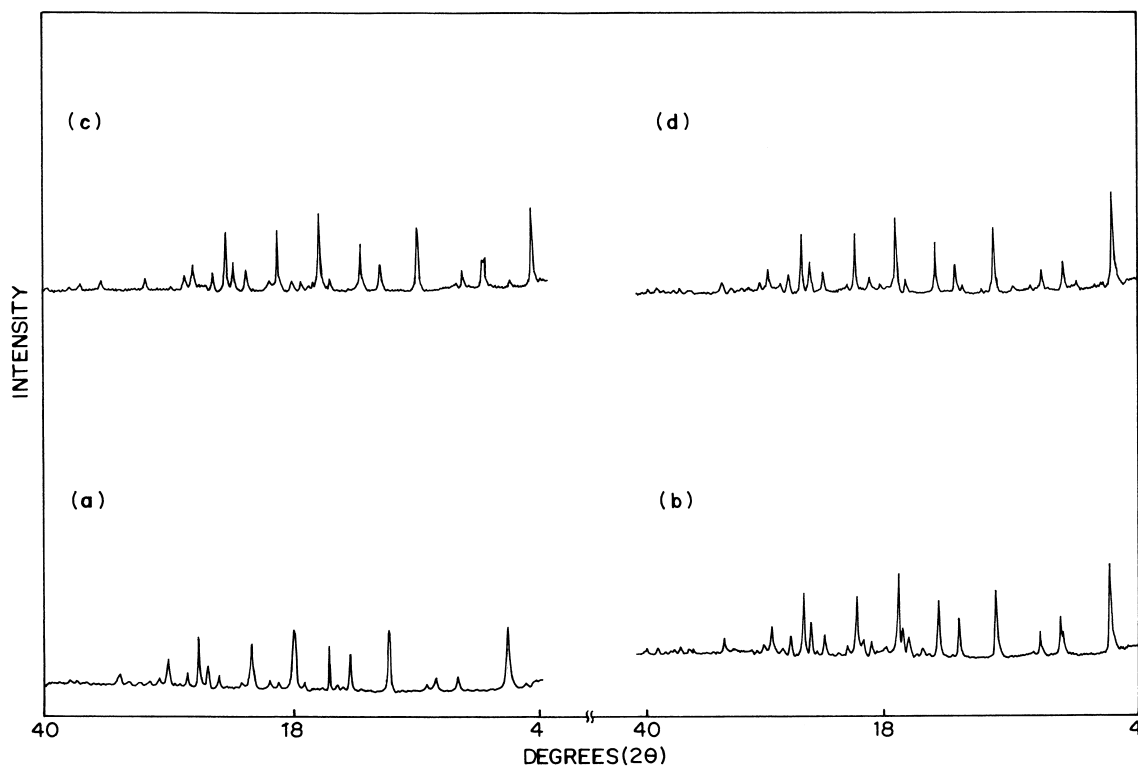
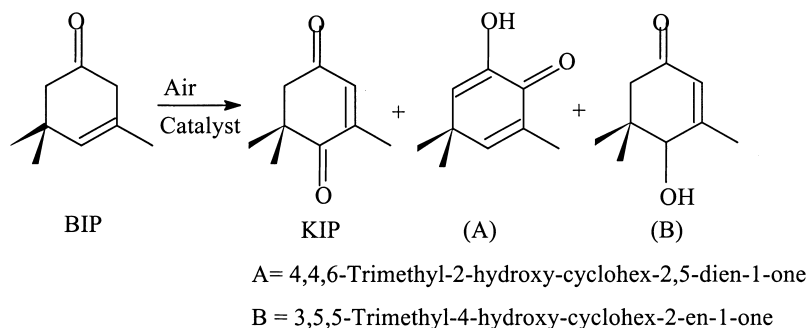


Fig. 1. Powder X-ray diffraction patterns: (a) Co(II)saloph-Y; (b) Co(II)Cl-saloph-Y; (c) Co(II)Br-saloph-Y and (d) Co(II)nitro-saloph-Y.

Scheme 2. Reaction scheme of oxidation of β -isophorone.

3.6. Catalytic activity

The zeolite encapsulated Co(II)saloph and their neat complexes oxidized BIP to KIP at ambient temperature and pressure of air. Neat as well as encapsulated catalysts gave KIP as the major product of oxidation along with side products A and B, as shown in the following reaction (Scheme 2). The selectivity for KIP was (>60%) at BIP conversion (>90%). However, the selectivity for KIP was highest (>95%) at BIP conversion in the range up to 30% and then decrease at higher conversions of BIP. The experimental conditions and the results obtained are presented in Table 3.

Catalytic activities of neat and encapsulated Co(II) catalysts in the oxidation of BIP were monitored as a function of time. Graphs of Conversions versus time for Co(II) neat and encapsulated catalysts are as shown in Figs. 2 and 3, respectively. It is seen from the graphs that conversion of BIP is exponentially changing with time.

From the catalytic activities data (Table 3), it is found that zeolite encapsulated catalysts gave higher conversions of BIP (TON's) than their corresponding

neat complexes. The higher activity of encapsulated complexes is because of site isolation of the complexes inside the zeolite cages. A conversion of BIP greater than 60% was obtained over a period of 3 h for neat and encapsulated complexes. Among the catalysts studied, Cl-saloph derivative of Co(II) gave the maximum BIP conversion followed by bromo- and nitro-substituted salophs. Similarly, the same trend is seen with their corresponding encapsulated catalysts. The increase in activities shown by the catalysts containing electronegative substituents on the saloph ligand was attributed to the stabilization of the corresponding cobalt superoxo radical (Co(III)–O–O \cdot) in neat as well as encapsulated forms during the chain radical oxidation of BIP. The order of reactivities of neat and encapsulated catalysts was in the following order:

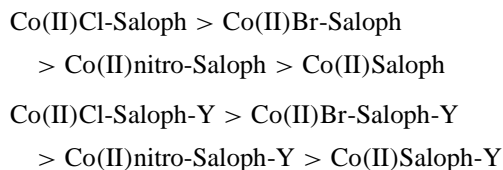


Table 3
Catalytic activities of neat and zeolite encapsulated complexes^a

Neat complexes	BIP conversion (wt.%)	TON ^b	Encapsulated complexes	BIP conversion (wt.%)	TON ^b
Co(II)Cl-saloph	15.3	29.8	Co(II)Cl-saloph-Y	25.8	50.3
Co(II)Br-saloph	12.5	24.2	Co(II)Br-saloph-Y	23.4	45.5
Co(II)nitro-saloph	10.8	21.0	Co(II)nitro-saloph-Y	20.6	40.1
Co(II)saloph	7.4	14.3	Co(II)saloph-Y	15.7	30.5

^a Conditions: BIP = 1 g (0.0072 mol); acetyl acetonate = 0.12 g; triethyl amine = 0.12 g; MEK = 8.0 g; temperature = 298 K; Co(II) catalysts; neat = 0.015 g; Co(II) encapsulated = 0.2 g; oxidant, air = 1 atm and reaction time = 1.0 h.

^b TON = mole BIP converted per mole of cobalt.

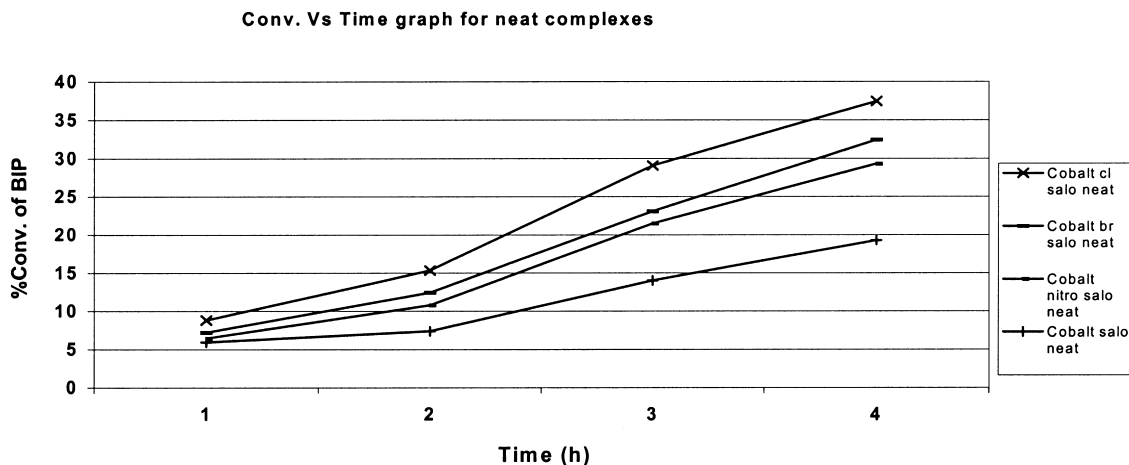


Fig. 2. Conversion of BIP vs. time plot for neat Co(II) complexes. Conditions: BIP = 1 g (0.0072 mol); acetyl acetonate = 0.12 g; triethyl amine = 0.12 g; MEK = 8.0 g; temperature = 298 K; Co(II) catalysts; neat = 0.015 g; oxidant, air = 1 atm.

3.7. Kinetic study of Co(II)Cl-saloph-Y neat complex catalyzed oxidation of BIP

The Co(II)Cl-saloph-Y catalyst was chosen for kinetic investigation as it is the most reactive catalyst system in the oxidation reaction. The kinetics of the oxidation of BIP to KIP catalyzed by Co(II)Cl-saloph-Y was investigated by varying the

concentrations of catalyst, substrate, oxidant (air), and temperature. Product samples were withdrawn at different time intervals and moles of BIP oxidized were estimated from the gas chromatographic analysis. The rates of oxidation of BIP were evaluated graphically from the moles of BIP converted as a function of time in all the experiments. The kinetic rate data is presented in Table 4.

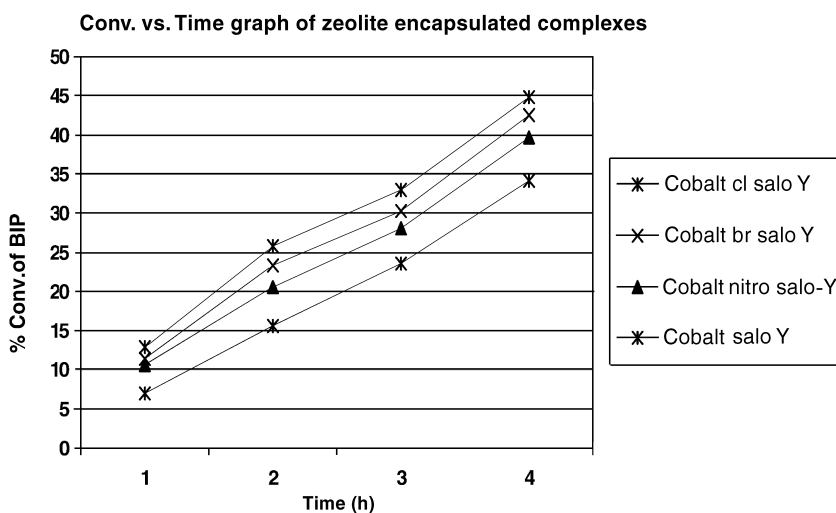


Fig. 3. Conversion of BIP vs. time plot of encapsulated Co(II) complexes. Conditions: BIP = 1 g (0.0072 mol); acetyl acetonate = 0.12 g; triethyl amine = 0.12 g; MEK = 8.0 g; temperature = 298 K; Co(II) encapsulated = 0.2 g; oxidant, air = 1 atm.

Table 4
Kinetic results of Co(II)Cl-saloph-Y catalyzed oxidation of BIP to KIP^a

Run no.	Co(II)Cl-saloph-Y concentration (mmol)	BIP concentration (mol)	O ₂ (air) (atm)	Temperature (K)	Rate of oxidation ($\times 10^4$ mol/h)
Effect of catalyst concentration					
1	0.0370	0.0072	1.0	303	1.75
2	0.0305	0.0072	1.0	303	1.40
3	0.0204	0.0072	1.0	303	1.00
4	0.0100	0.0072	1.0	303	0.41
Effect of BIP concentration					
5	0.0370	0.0145	1.0	303	18.0
6	0.0370	0.0217	1.0	303	22.0
7	0.0370	0.0290	1.0	303	27.0
8	0.0370	0.0360	1.0	303	36.0
Effect of temperature					
9	0.0370	0.0145	1.0	293	10.0
10	0.0370	0.0145	1.0	303	18.0
11	0.0370	0.0145	1.0	313	32.0
Effect of air (O ₂) pressure (volume reaction mixture = 30 ml)					
12	0.11	0.0217	1.0	303	22.0
13	0.11	0.0217	7.0	303	28.0
14	0.11	0.0072	14.0	303	34.0

^a Conditions: acetyl acetonate = 0.12 g; triethyl amine = 0.12 g and MEK = 8.0 g.

3.8. Mechanistic studies

3.8.1. UV–VIS spectroscopy

Mechanistic studies of oxidation of BIP were performed using neat Co(II)saloph by UV–VIS spectroscopy. The UV–VIS spectra of Co(II)saloph was taken in MEK solvent and it showed an absorption maximum at 450 nm (Fig. 4), which is characteristic of Co(II) species having a square planar configuration. When the catalyst solution was interacted with air, the absorption maximum was shifted to higher wavelength 456 nm, showing the formation of new Co(III)–O–O• superoxo species. When, the substrate was added to this solution, the absorption maximum shifted further to 500 nm, suggesting a complex formation through peroxo linkage. The mechanism proposed for the oxidation of BIP to KIP catalysed by Mn(III) Salen under homogeneous conditions was similar to the one proposed in Scheme 3, wherein, Mn(IV) metalloperoxy intermediate has been proposed as the intermediate species in the oxidation of BIP catalyzed by Mn(III)Cl-Salen under homogeneous conditions [13].

3.8.2. Kinetics and rate law

Based on the kinetic data (Table 4) and mechanistic studies carried out by UV–VIS spectroscopy, a probable mechanism for Co(II) catalyzed oxidation of BIP to KIP has been given in Scheme 3.

The proposed mechanism in Scheme 3 involves the reaction between two moles of LCo(II) catalyst precursor with one mole of oxygen in a pre-equilibrium step to give LCo(III)–O–O• superoxo intermediate species 'a' and LCo(II). The formation of species 'a' is a well-established in literature [15]. The formation of species 'a' has been observed by UV–VIS spectra, when catalyst solution was interacted with air (O₂) and an absorption maximum of 456 nm was observed (Fig. 4). The shift in the absorption maximum from 456 nm (catalyst solution + O₂) to 501.5 nm further with the addition of BIP was attributed to the formation of LCo(III)–O–O• superoxo intermediate. Species 'a' being reactive, it immediately takes up a mole of BIP in another pre equilibrium step to form a π -bonded intermediate species 'b'. In a rate determining step, cyclic peroxometallation takes place to form cyclometalloperoxy species 'c'. This in a fast step forms species

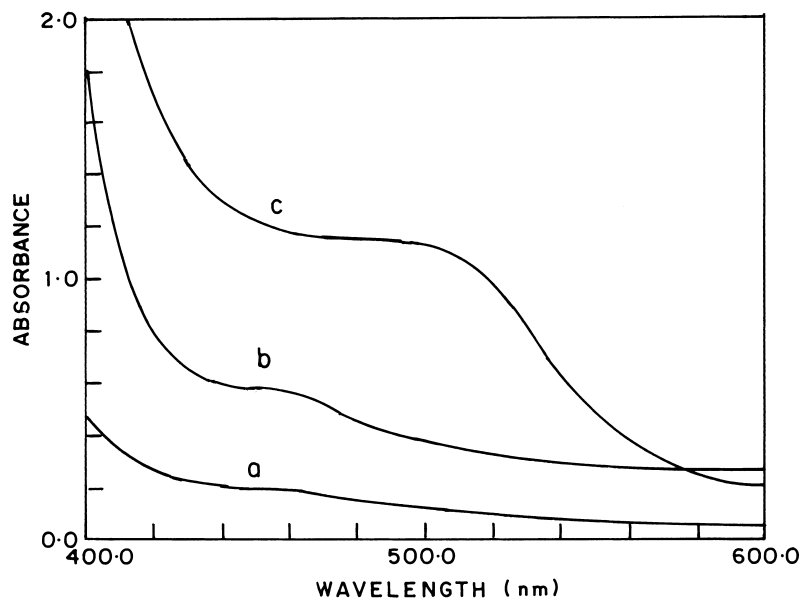
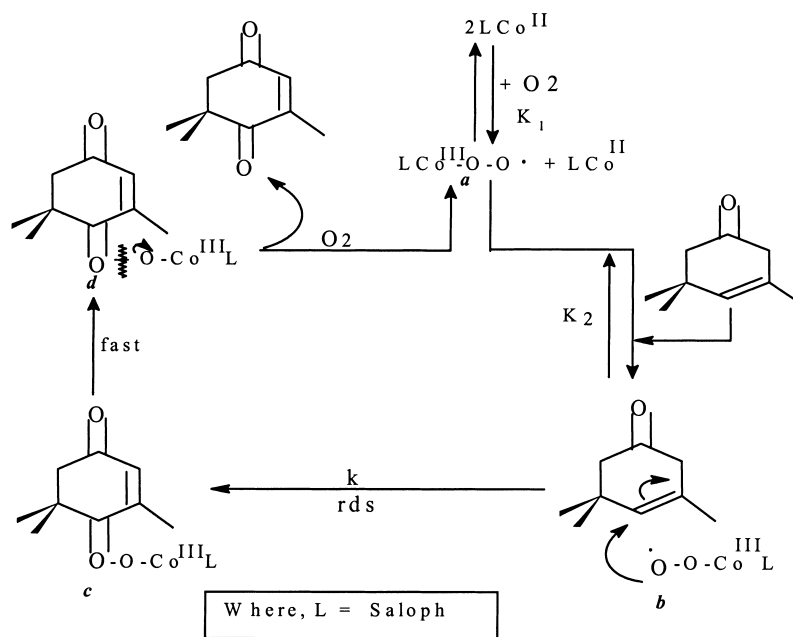


Fig. 4. UV-VIS spectra: (a) Co(II)saloph neat in CH_3CN ; (b) Co(II)saloph + air and (c) Co(II)saloph + air + BIP.



Scheme 3. Mechanism.

d, which undergoes homolytic cleavage by transfer of oxygen and double bond migration to give KIP, while regenerating the active catalytic species *a* in presence of air to continue the catalytic cycle. Similar mechanisms have been proposed for the oxidation of styrene [16] and octene [17] and the oxidation of BIP to KIP [13]. However, in the proposed mechanism, the role of solvent MEK, acetyl acetonate and triethyl amine has not been investigated and additives seem to stabilize the catalytic intermediates in the oxidation reaction.

3.8.3. Rate law

From the results presented in Table 2, it is found that, the rates of oxidation of BIP to KIP had a first-order dependence with respect to catalyst and BIP concentrations (determined graphically) and one and half order dependence with respect to oxygen concentration. Based on kinetic dependence studies and the mechanism shown in Scheme 3, the overall rate equation for the oxidation of BIP to KIP catalyzed by LCo(II) catalyst systems could be represented as

$$\text{rate} = k_r K_1 K_2 [\text{catalyst}] [\text{BIP}] [\text{O}_2]^{1/2} \quad (1)$$

where the concentrations of the reactants are represented in square brackets and k_r , K_1 and K_2 are pseudo-second-order rate constant and preequilibrium constants of the first and second steps (Scheme 3), respectively. The values of k_r , K_1 and K_2 were calculated graphically by a standard method using steady state conditions of the oxidation reaction. These values are $k_r = 20.8 \text{ min}^{-1}$, $K_1 = 80.5 \text{ M}^{-1}$ and $K_2 = 154.6 \text{ M}^{-1}$, respectively. The value of K_2 is twice higher than K_1 , which indicated that the superoxo species *a* is less stable than the mixed ligand π -bonded intermediate species *b* and hence the formation of cyclometalloperoxo species *c* from species *b* takes place in a rate determining step.

From the temperature dependence study, the rates of oxidation of BIP determined were plotted as $-\ln(\text{rate})$ versus $1/T$ (Arrhenius plot, Fig. 5) and from the slope of the straight line, the activation energy evaluated was 12.3 kcal/mol.

Thermodynamic activation parameters are of importance in knowing the influence of temperature over the performance of the catalyst in any catalytic transformations. Standard thermodynamic relations were used to calculate thermodynamic activation parameters and

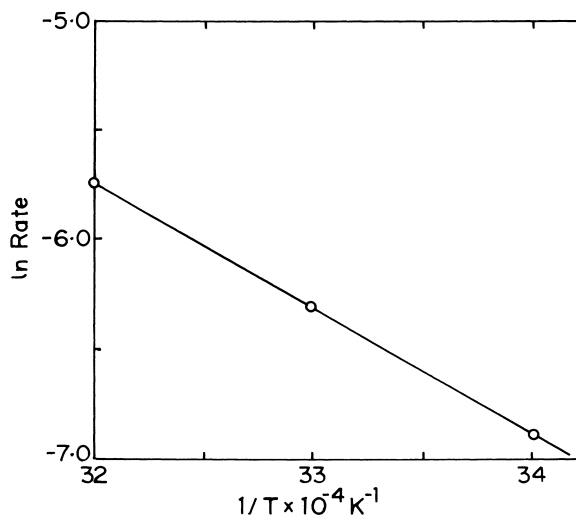


Fig. 5. Arrhenius plot.

these are:

1. Slope of the Arrhenius graph = $-E_a/R$. (2)
2. Enthalpy of activation, $\Delta H^\ddagger = E_a - RT$. (3)
3. Entropy of activation,

$$\Delta S^\ddagger = \frac{\Delta H^\ddagger + Rh/k \ln k_r}{T} \quad (4)$$

4. Gibb's free-energy of activation,

$$\Delta G^\ddagger = \Delta H^\ddagger - T \Delta S^\ddagger \quad (5)$$

where E_a = energy of activation, ΔH^\ddagger = enthalpy of activation, ΔS^\ddagger = entropy of activation, ΔG^\ddagger = free-energy of activation, R = gas constant, T = temperature in K, h = Planck's constant, k = Boltzman's constant and k_r = pseudo-second-order rate constant of the reaction.

Thermodynamic activation parameters evaluated for Co(II)Cl-saloph-Y catalyzed oxidation of BIP to KIP are; $E_a = 12.3 \text{ kcal/mol}$, $\Delta H^\ddagger = 11.7 \text{ kcal/mol}$, $\Delta S^\ddagger = +40.5 \text{ cal}^\circ \text{ mol}$ and $\Delta G^\ddagger = -0.57 \text{ kcal/mol}$. These values indicated that the oxidation of BIP by molecular oxygen to KIP catalyzed by Co(II)Cl-saloph-Y is exothermic reaction with negative free energy. The negative ΔG^\ddagger values indicated that the reaction is feasible at lower temperatures in presence of the above catalyst system. Enthalpy and +ve entropy values are indicative of bond rearrange-

ment in the oxidation reaction mechanism as shown in Scheme 3.

4. Conclusions

Zeolite encapsulated Co(II)saloph complexes catalyzed the oxidation of BIP with molecular oxygen to KIP with higher selectivity (>60%) at BIP conversion (>90%). Encapsulated catalyst systems showed higher activities than their homogeneous analogues in the oxidation reaction. Mechanism of oxidation catalyzed by LCo(II) revealed that the transfer of oxygen to BIP to form KIP took place via LCo(III)–O–O[•] superoxo intermediate species. The encapsulated catalysts were recycled with Co(II)Cl-saloph-Y catalyst as a representative and were found that the catalyst was active in the oxidation reaction in few cycles studied.

Acknowledgements

One of the authors Trissa Joseph thanks Dr. C. Gopinathan for useful discussions in the research work and CSIR, New Delhi for awarding a Senior Research Fellowship to carry out this work.

References

- [1] Y. Iwasawa, Tailored Metal Catalysts, Reidel, Holland, 1986.
- [2] A. Kozlov, K. Asakura, Y. Iwasawa, Macroporous Masoporous Mater. 21 (1998) 579.
- [3] M. Ichikawa, Platinum Metals Rev. 44 (2000) 3.
- [4] K.J. Balkus Jr, A.K. Khanmamedova, K.M. Dixonand, F. Bedioui, Appl. Catal. A: Gen. 143 (1996) 159.
- [5] C. Bowers, P.K. Dutta, J. Catal. 122 (1992) 271.
- [6] R.F. Parton, I.F.J. Vankelecom, M.J.A. Casselman, C.P. Bezoukhanova, J.B. Uytterhoeven, P.A. Jacob, Nature 370 (1994) 541.
- [7] N. Herron, J. Coord. Chem. 19 (1986) 25.
- [8] N. Herron, Inorg. Chem. 25 (1988) 4714.
- [9] C.R. Jacob, S.P. Varkey, P. Ratnasamy, Appl. Catal. 168 (1998) 353.
- [10] S.P. Varkey, C. Ratnasamy, P. Ratnasamy, J. Mol. Catal. 135 (1998) 295.
- [11] C.R. Jacob, S.P. Varkey, P. Ratnasamy, Appl. Catal. 182 (1999) 353.
- [12] T. Joseph, C.S. Sajanikumari, S.S. Deshpande, S. Gopinathan, Indian J. Chem. 38A (1999) 792.
- [13] S.B. Halligudi, K.N. Kala Raj, S.S. Deshpande, S. Gopinathan, J. Mol. Catal. 2554 (2000).
- [14] S.B. Halligudi, S.S. Deshpande, M.P. Degaunkar, CSIR, Patent, Filed.
- [15] El.-S.A. Aly, J. Mol. Catal. 78 (1993) L1.
- [16] A. Nishinaga, T. Yamada, H. Fujisawa, K. Ishizaki, H. Ihara, T. Matsuura, J. Mol. Catal. 48 (1988) 249.
- [17] O. Brotolini, F.D. Furia, G. Modena, R. Seraglia, J. Mol. Catal. 22 (1984) 313.